

## Highly solar active green oxidant combined W, N codoped ZnO powder: Synthesis Characterization and Photocatalytic Degradation of textile Dye

Umadevi M and Jenif D'Souza A\*

Department of Chemistry, Prist deemed to be University, Puducherry campus, Puducherry, India.

\*Corresponding Author: E-Mail: dsouzajenif@gmail.com

Received: 18<sup>th</sup> Dec 2020, Revised and Accepted: 24<sup>th</sup> Dec 2020

### ABSTRACT

The photocatalytic activity of W, N-codoped ZnO was tested by the degradation of Reactive Blue 4 (RB 4) under renewable solar light irradiation. A series of W, N-codoped ZnO photocatalyst with different mole ratio (0.02 mol%, 0.03 mol%, 0.04 mol%, 0.05 mol%, and 0.06 mol%) were prepared sol-gel technique. The pure ZnO was low photocatalytic activity, due to its poor surface properties, gets photocorrosion and low utilization of visible light. These problems were minimised by doping with W and N on ZnO. The photocatalytic activity of W, N-codoped ZnO was remarkably higher than that of the as-prepared sample like pure ZnO. The highlighted photocatalytic properties of W, N-codoped ZnO were confirmed by XRD, SEM and UV-DRS, PL and FTIR analysis. W, N-codoped TiO<sub>2</sub> photocatalyst has photostability and long durability.

**Keywords:** W, N-Codoped ZnO, sol-gel route, Photocatalytic Degradation, Reactive Blue 4 and solar Light.

### 1. INTRODUCTION

In the past eras, a significant scientific improvement and increasing human residents, which was due to various annoying human activities. Conversely, the evolution of industrialized enlargement has conveyed to make environmental pollution, lead to unsafe for humans and their surroundings<sup>[1]</sup>. Due to this pollution, human receives major diseases like chronic illness, skin diseases, different types of cancers and neurobehavioral disorders, etc

Among the water pollutants, synthetic dyes are possessing major issues. Synthetic dyes are commonly used by various industries, especially textile ones. These physically and chemically stable compounds are harmful to the environment. Synthetic dyes are recalcitrant compounds that exhibit high solubility in water and accumulate in both wastewater and industrial effluents<sup>[2,3]</sup>. So that, the recovery of wastewater by conventional methods is not suitable for emergent pollutants<sup>[4,5]</sup>. Heterogeneous photocatalysis can be satisfactorily applied for the decontamination of natural samples through the photocatalytic degradation of toxic pollutants

from complex matrices, such as river water and wastewater<sup>[6]</sup>. All renewable technologies have become a promising alternative for both energy generation and wastewater treatments. Solar photocatalysis is a suitable option to degrade recalcitrant pollutants from water<sup>[7,8]</sup>.

The absorption of a photon initiates the photodecomposition of semiconductor with energy greater than or equal to the bandgap of semiconductor producing electron-hole pairs<sup>[9]</sup>. It is important for prolonging electron-hole recombination before a designated chemical reaction occurs on the semiconductor surface. Several semiconductor photocatalysts such as TiO<sub>2</sub>, ZnO, WO<sub>3</sub>, SnO<sub>2</sub>, CdS, and ZnS<sup>[10]</sup> have been used for the treatment of wastewater pollutants under visible light irradiation. Among semiconductors, zinc oxide (ZnO) has attracted attention due to its environmental stability as compared to other metal oxides<sup>[11]</sup>. Application of photocatalysis, especially using semiconductors such as ZnO, appears to be a more appealing approach than the conventional chemical oxidation methods for decomposition of toxic compounds to nonhazardous product<sup>[12]</sup>. This is

because semiconductors has novel properties such as inexpensive, non-toxic, high surface area, broad absorption spectra and affording facility for the multi-electron transfer process. ZnO has been demonstrated as an improved photocatalyst as compared to commercialized TiO<sub>2</sub> based on its more significant initial rate of activities and higher absorption efficacy of solar radiations<sup>[13]</sup>. However, ZnO has almost the same bandgap as TiO<sub>2</sub>. Surface area and surface defects play an essential role in the photocatalytic activities of metal oxide. The photocatalytic activity of ZnO is restricted to the irradiation wavelengths in the UV region because of its wide bandgap of about 3.2 eV and low quantum efficiency<sup>[14]</sup>. The wide bandgap and fast electrons recombination of ZnO constrains its application. Some alternative strategies to extend ZnO photoresponse in the visible light region are: (a) ZnO doping<sup>[15]</sup>, (b) co-doping [16], (c) coupling with lower band gap semiconductors<sup>[17]</sup>, (d) surface plasmon resonance<sup>[18]</sup>, (e) quantum dots<sup>[19]</sup>, and (f) sensitization with natural and synthetic dyes<sup>[20]</sup>.

Several attempts also have been made to improve the efficiency of photocatalysts by using doping materials. Doping is required to improve the efficiency of photocatalysts. The reduction of the optical energy gap of ZnO by doping is an advantage for use in optoelectronic devices. Among these doping materials, Ag-doped ZnO<sup>[21]</sup>, N-doped ZnO<sup>[22]</sup>, Mg-doping on ZnO<sup>[23]</sup> shows good photocatalytic activity.

Doping of non-metallic elements can form an intermediate energy level in the band gap of ZnO, which can reduce the band gap of ZnO and increase the photocatalytic activity of visible light. Anion doping can achieve better optical response of ZnO, especially in V group elements N, P, As<sup>[24]</sup>. Substitution by N doping is one of the best way to lower down the band gap of ZnO, owing to the atomic size and electronegativity of the non-metal element N are the closest to O atom<sup>[25]</sup>, and the mixing p state of N and 2p state of O narrow the band gap of semiconductor oxide<sup>[26]</sup>. Furthermore, the introduction of N atoms into ZnO lattice will bring the energy band into intermediate energy level and reduce the absorption energy, which can increase photocatalytic activity<sup>[27]</sup>.

The combination between the properties of the nonmetals with that of transition metals may induce desirable optical and photocatalytic properties in ZnO. The integration between the visible-light responsive properties of nonmetal and the metal as trap centers can prompt more efficiency for practical applications. A. M. Youssef and S. M. Yakout designed effective visible light photocatalysts composed of C/La or Ce codoped

ZnO nanostructures were prepared by sol gel method.

Based on the literature reviews, we have interestingly focused in the codoping technique on the ZnO photocatalysts. In this research work, highly solar active W, N co-doped ZnO were synthesised. Nitrogen and tungsten ion was doped on ZnO by annealing treatment under urea and ferrous sulphate heptahydrate solution. The as-prepared sample could efficiently overcome the drawbacks mentioned above to some extent, because it has high surface area, effective charge separation and ability to absorb light at visible light region. The W, N co-doped ZnO structures with high surface area can provide an excellent support for active sites due to pore sizes and volume. Photocatalytic activity of the W, N co-doped ZnO was investigated by monitoring the degradation of Reactive Blue 4 under solar light irradiation.

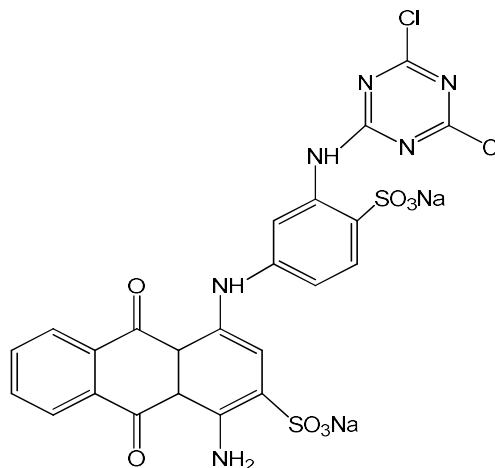
## 2. MATERIALS AND METHOD

### 2.1. Chemicals used

Zinc chloride (GR), Sodium tungstate (GR), Urea and sodium bicarbonate (GR) were used as such for the preparation of the W, N codoped ZnO photocatalyst. Sodium hydroxide and Hydrochloric acid (AR) were used for modifying the pH of the solutions. Hydrogen Peroxide 30% W/V (Qualigens) was used as oxidant. Potassium dichromate (AR), Silver sulphate (GR), Mercury sulphate (GR), 99% Ferroin (GR) and Sulphuric acid were used for COD analysis. Double distilled deionised water was used for the preparation of the dye solutions.

The photocatalytic degradation of reactive dye like reactive blue 4 (Molecular Weight: 683.41,  $\lambda_{\max}$ : 598 nm, abbreviation: RB 4) have been studied on W, N codoped ZnO and its parent photocatalysts.

The chemical structure of RB 4 was given bellow.



Chemical structure of Reactive Blue 4

## 2.2. Preparation of W, N- codoped ZnO photocatalyst

10 g of zinc chloride and 0.01 mol% of Sodium tungstate and Urea were dissolved in 100 ml of double distilled water for the preparation of W, N- codoped ZnO photocatalyst. The dopant concentrations were added the ratios like 0 to 0.05 mol percentage. To that solution required amount of sodium bicarbonate was then added in portions with vigorous stirring for several minute, finally the precipitate was formed. The doped photocatalysts are washed several times with distilled water to remove NaCl formed. The precipitate was then dried at 100°C to remove the water. The obtained precipitate was grinded in an agate mortar and pressed into a ceramic crucible. The material was calcinated at 500°C for 4 hrs. The undoped ZnO was also synthesized in the same procedure without adding dopant concentration.

## 2.3. Characterization

X-ray powder diffraction (XRD) patterns of the photocatalysts were recorded on a Philips X'pert-MPD diffractometer in the  $2\theta$  range 20–80° using Cu-K $\alpha$  radiation. The data were collected with a step of 0.028 ( $2\theta$ ) at room temperature. The phase structure of the products was determined by comparing the experimental X-ray powder patterns to the standard compiled by the Joint Committee on Powder Diffraction and Standards (JCPDS). The crystallite sizes were calculated from the peak width using the Scherrer equation. The surface morphologies and particle size were observed by Scanning Electron Microscopy (JEOLJSM-6360LV). UV-Visible diffuse reflectance spectra were developed by a Perkin-Elmer Lambda 35 spectrometer. BaSO<sub>4</sub> was used as the reflectance standard. The photoluminescence emission spectra of the samples were measured at room temperature using Perkin-Elmer LS 55 Luminescence spectrophotometer. Fourier Transformer Infra Red data were collected over the spectral range 400-4000 cm<sup>-1</sup> with a BRUKER IR spectrometer equipped with a 5 cm integrating sphere (Labsphere). KBr was used as a reference material, and the data were transformed into transmittance.

## 2.4. Photocatalytic studies

### 2.4.1. Photocatalytic degradation study of RB 4

All the photocatalytic experiments were performed under natural sunlight on clear sky days during the period of June to October-2020. In a typical experiment, 50 ml of dye solution (concentration 50 mg l<sup>-1</sup>) was taken with 50 mg of photocatalyst in a 250 ml glass beaker. Then the

dye solution was kept in direct sunlight with continuous aeration and the concentration of the dye remains was measured periodically by measuring its light absorbance at the visible  $\lambda_{max}$  by using Elico SL-171 Visible spectrophotometer. In order to avoid the variation in results due to fluctuation in the intensity of the sunlight, a set of experiments have been carried out simultaneously. For pH studies the pH of the dye solutions were modified to different values (3, 5, 7, 9 and 12) by using 0.1M HCl and NaOH solution.

### 2.4.2. Chemical Oxygen Demand Analysis

The chemical oxygen demand (COD) is the indirect measurement of the oxygen needed for the complete oxidation of all the compounds present in solution. The COD of the degraded dye solution were analyzed in standard dichromate method. For the analysis, 0.4g of H<sub>2</sub>SO<sub>4</sub> was added to 20ml of the degraded dye solution in a 250 ml round bottom flask. To that 10ml of 0.25N K<sub>2</sub>Cr<sub>2</sub>O<sub>7</sub> was added and mixed well. Then 30 ml of H<sub>2</sub>SO<sub>4</sub>-AgSO<sub>4</sub> reagent (prepared by dissolving 0.5g of AgSO<sub>4</sub> in 30ml of Concentrated H<sub>2</sub>SO<sub>4</sub>) was added slowly with constant stirring. After that few pieces of pumice stones where added and the flask was fitted with a condenser and reflux for 2 hours. The solution was cooled and diluted to 150ml with distilled water and the entire content was titrated against 0.25N Ferrous Ammonium Sulphate (FAS) solution using ferrion as indicator.

$$\text{COD in mg l}^{-1} = \frac{(V_1 - V_2) \times N \times 8}{x}$$

Where V<sub>1</sub> & V<sub>2</sub> are the volume of FAS solution consumed for blank and test sample respectively, N is the normality of FAS solution and x is the volume of sample taken for analysis

## 3. RESULTS AND DISCUSSION

### 3.1 Physicochemical characterization of the photocatalyst

#### 3.1.1 X-ray diffraction studies

The powder XRD patterns of ZnO and 0.04 mol% W, N- codoped ZnO were as shown in **Figure 1**. Both samples were identified a single phase wurtzite ZnO by XRD analysis (JCPDS card nos.: 89-1397; 89-0511; 36-1451). The W, N codoped ZnO shows high intensity of the peaks, indicates that ZnO are high crystallinity<sup>[28]</sup>. On the other hand codopants such as W and N incorporation on ZnO lattice increased the crystallinity. The mean crystallite sizes of the samples calculated by using the Scherrer formula for ZnO and W, N- codoped ZnO was given in the **Table 1**. The result shows that W, N doping decreases the particle size of the ZnO. An XRD pattern of W, N- codoped ZnO indicates the

uniform dispersion of W and N ions. Moreover the bulk structure remains virtually unchanged by the W and N- incorporation<sup>[29, 30]</sup>.

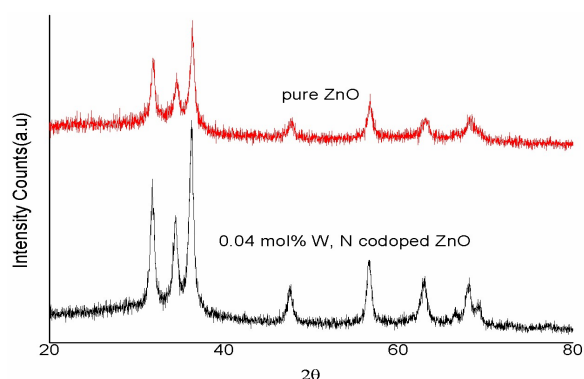


Figure - 1: XRD patterns of ZnO and W, N-codoped ZnO.

Table - 1: XRD calculation results of ZnO and W, N-codoped ZnO

Photocatalyst	$d_{(101)}$ -spacing (Å)	Full Width Half Maximum	Average crystallite size (nm)
ZnO	2.4753	0.342°	73
0.04% W, N-codoped ZnO	2.4710	0.400°	38

### 3.1.2. SEM analysis of the photocatalyst

The SEM micrographs of ZnO and 0.04% W, N- codoped ZnO photocatalyst were shown in **Figure 2 a,b** respectively. The micrographs show that ZnO particles have blunder particle morphology whereas W, N- codoped ZnO has irregular arrangement patterns composed of spherical of ZnO. This type of morphology could be able to completely degrade dye solutions. The reason is doped photocatalyst have shown highly rough surface.

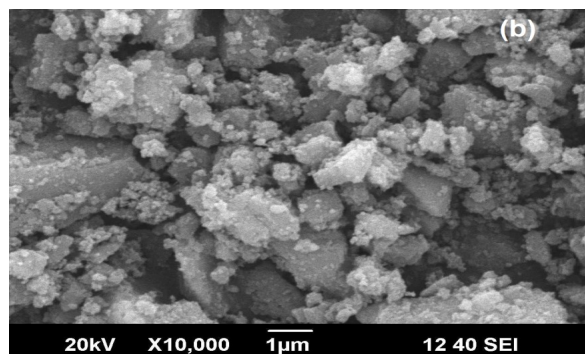
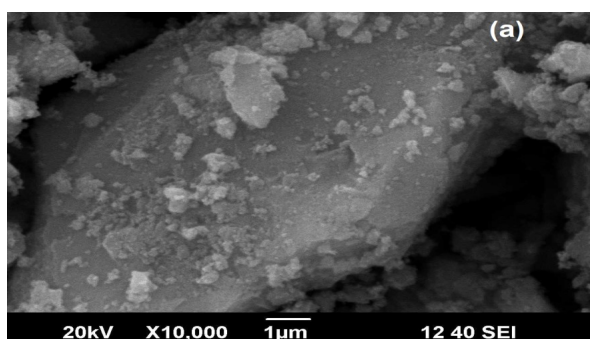


Figure - 2: SEM micrograph of (a) ZnO, (b) 0.04 % W, N codoped ZnO photocatalyst.

### 3.1.3. Diffused Reflectance UV-Visible analysis of the photocatalyst

Diffused reflectance spectra UV-visible spectra of ZnO and W, N- codoped ZnO were given in **Figure 3**. The results show that the absorption onset of ZnO and W, N-codoped ZnO were 390 nm and 480 nm respectively. Therefore W, N-codoped ZnO can utilize visible light than the pure ZnO for photoexcitation process and expected to have more activity in the solar radiation than the undoped ZnO. The red shift in the light absorption of ZnO on W and N doping has been interpreted by Kim et al., as the sp-d exchange interaction between the band electrons and the localized “d” electrons of the transition metal ion at the cationic site<sup>[31]</sup>.

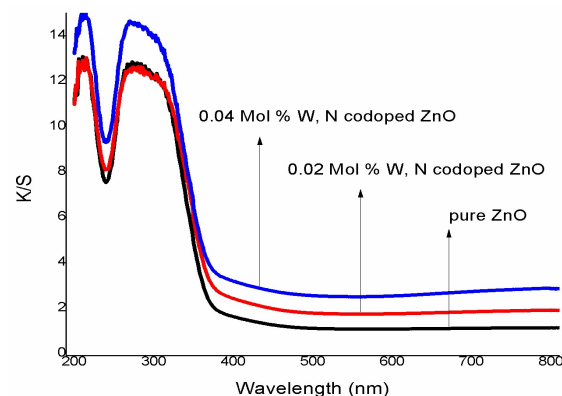


Figure - 3: Diffused Reflectance UV-Visible spectra of ZnO and W, N-codoped ZnO.

### 3.1.4. Photoluminescence spectra

To study the optical properties of the synthesized solar active W, N codoped ZnO the PL spectrum is recorded at room temperature. The PL spectrum compared with pure ZnO powder and W, N codoped ZnO are shown in **Figure 4**.

The UV emission located at 391 nm is the band-edge emission resulting from the recombination of free excitons, and the broad green emission centered at 451 nm is caused by

the radiative recombination of the photogenerated holes with electrons around the surface oxygen vacancy. In comparison with the PL spectrum of as prepared ZnO, the UV emission of W, N codoped ZnO is enhanced, while the electron hole recombination might be suppressed. This phenomenon can be attributed to the reduction of band gap energy while doping W and N. The similar observation has been reported previously<sup>[32]</sup>.

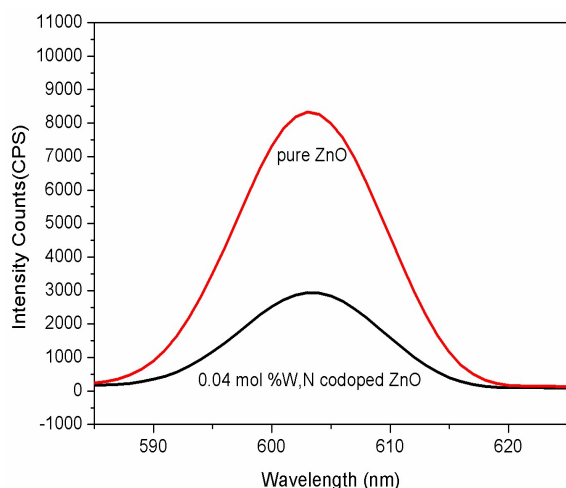


**Figure - 4:** Photoluminescence spectrum of pure ZnO and 0.04 mol% W, N codoped ZnO

### 3.1.5 FT-IR Spectroscopic analysis

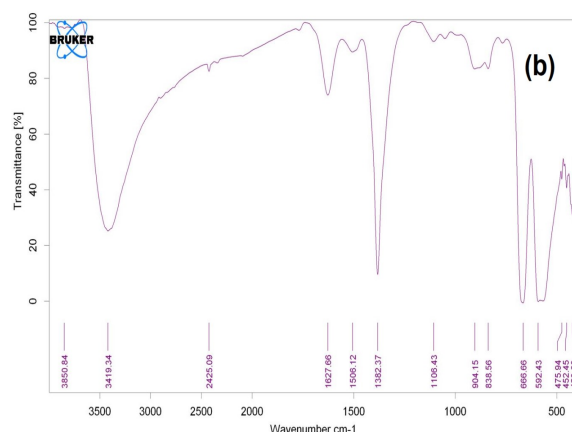
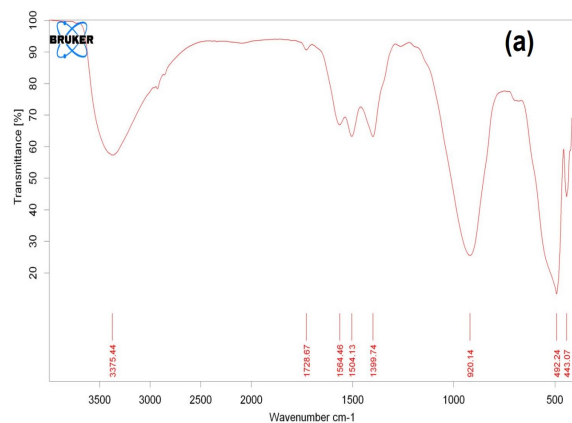


**Figure - 5:** FT-IR spectra of (a) pure ZnO and (b) 0.04 mol% W, N-codoped ZnO photocatalyst.

Fourier transforms infrared spectroscopy of the hydrolyzed particles (**Fig. 5**) show strong peaks at  $1564\text{ cm}^{-1}$  and at  $1399\text{ cm}^{-1}$ . The previously mentioned peak at  $1564\text{ cm}^{-1}$  indicates the formation of ZnO<sup>[33]</sup>. When tungsten doping with ZnO, the peak value shifted to 1627, this indicates O- W bond has elongated. Peaks at  $475\text{ cm}^{-1}$  and  $452\text{ cm}^{-1}$  correspond to N-O stretching and bending. These peaks confirm integration of tungsten (W) ion and nitrogen (N) with zinc (Zn) ion.

## 3.2. Photocatalytic Studies

### 3.2.1 Photocatalytic activity of W, N -codoped ZnO

The photocatalytic activity of the W, N-codoped ZnO photocatalysts has been evaluated from their activity in the degradation of Reactive Blue 4 (RB 4) in the presence of solar light. This dye has been chosen for the studies since it has a strong light absorption in UV-visible region. The UV-visible transmittance spectrum of the RB 4 solution show that more than 80% of incident light in the wavelength range 200-450 nm was absorbed by  $50\text{ mg l}^{-1}$  dye solution in a path length of 1 cm. Hence, the degradation of the RB 4 solution with concentration above  $50\text{ mg l}^{-1}$  in a simple photocatalytic process over a UV active photocatalyst like ZnO is difficult and will take more treatment time for complete degradation. The degradation of  $50\text{ mg l}^{-1}$  RB 4 on W, N-codoped ZnO in a photocatalytic process was shown in **Figure 6**. The results show that W, N-codoped ZnO have higher activity than pure ZnO in simple photocatalytic process. The W, N-codoped ZnO with 0.01 mol % W, N ion content has show maximum activity for the degradation of the dye and increase of W, N ion above 0.04 mol % decreases the activity of the ZnO. The high activity of the above 0.04 mol % W, N-codoped ZnO might be due to the better inhibition of electron-hole recombination. However, the rate of degradation

of the dye over 0.04 mol % W, N-codoped ZnO was steady and a complete degradation was achieved in 100 minutes of light irradiation. On the same experimental conditions pure ZnO needs 180 minutes for 99% degradation of the dye solution. This shows that the 0.04 mol % W, N-codoped ZnO is the most active material for the degradation of the RB 4 dye solution.

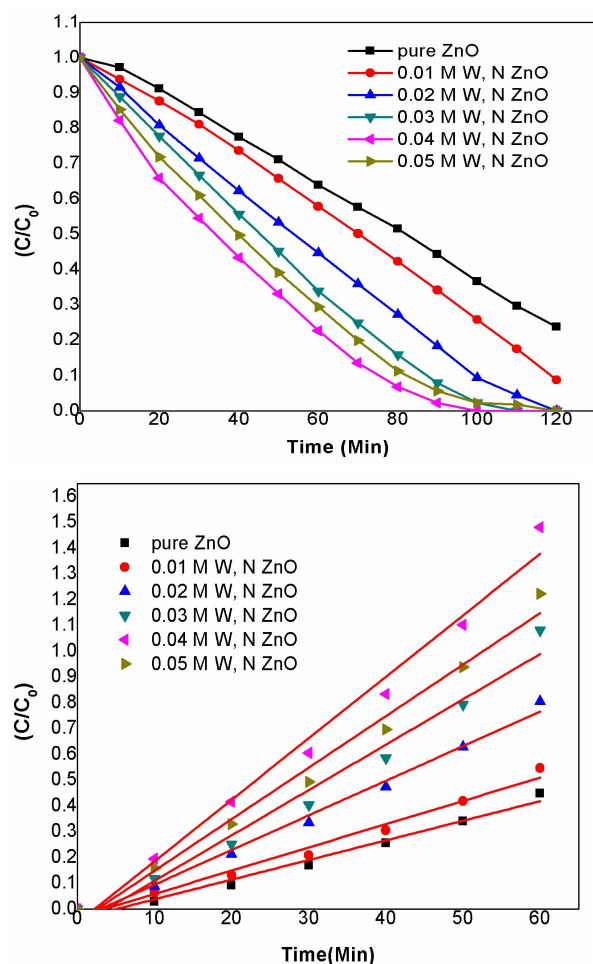


Figure - 6: Effect on the degradation and kinetic studies of RB 4 over W, N -codoped ZnO in Photocatalytic processes.

Analyses of these curves were carried out with the Langmuir- Hinshelwood kinetic model:

$$r_s = \frac{kKC}{(1+KC)}$$

Where,  $r_s$  is the specific degradation reaction rate of the dye ( $\text{mg l}^{-1} \text{min}^{-1}$ ),  $C$  the concentration of the dye ( $\text{mg l}^{-1}$ ),  $k$  the reaction rate constant ( $\text{s}^{-1}$ ) and  $K$  is the dye adsorption constant. When the concentration ( $C$ ) is small enough, the above equation can be simplified in an apparent pseudofirst - order equation.

$$(-dC/dt) = r = kKC = k_{app}C$$

After integration, we will get

$$-\ln(C/C_0) = k_{app}t$$

Where  $C_0$  is the initial concentration ( $\text{mg l}^{-1}$ ),  $C$  is the concentration of the dye after “ $t$ ” minutes of illumination. The data obtained from the degradation of RB 4 fits well with the apparent pseudofirst order kinetics.

### 3.2.2. Photocatalytic Mechanism

The probable role of W, N in ZnO photocatalyst was illustrated in the Figure 7. From the Figure, it could be seen that the W, N codoped ZnO photocatalyst could be simultaneously excited to form electron-hole pairs. Due to this band position, the photoexcited electron on the CB of ZnO can be abstracted by oxidant ( $\text{O}_2$ ). As a result, the electron and hole generated in the ZnO will have sufficient life time to prompt the photocatalytic oxidation reactions. However, the photogenerated electron in the CB of ZnO can react with oxidant such as oxygen molecule ( $\text{O}_2$ ) to produce  $\cdot\text{O}_2^-$  rather than undergoing recombination with holes in surface of ZnO. Then, the  $\cdot\text{O}_2^-$  react with  $\text{H}^+$  to give  $\text{HOO}\cdot$ , which subsequently react with dye molecule in the solution. The generated holes ( $\text{h}^+$ ) also reduced with water molecule ( $\text{H}_2\text{O}$ ) to produced active hydroxyl radical. These hydroxyl radicals degrade the dye solution. As a result, the photocatalytic activity of W, N codoped ZnO photocatalyst was much higher than that of the wide band gap semiconductor ZnO. Therefore, the enhancing photocatalytic activity of W, N codoped ZnO photocatalyst was most possibly related to the codoped ZnO structure.

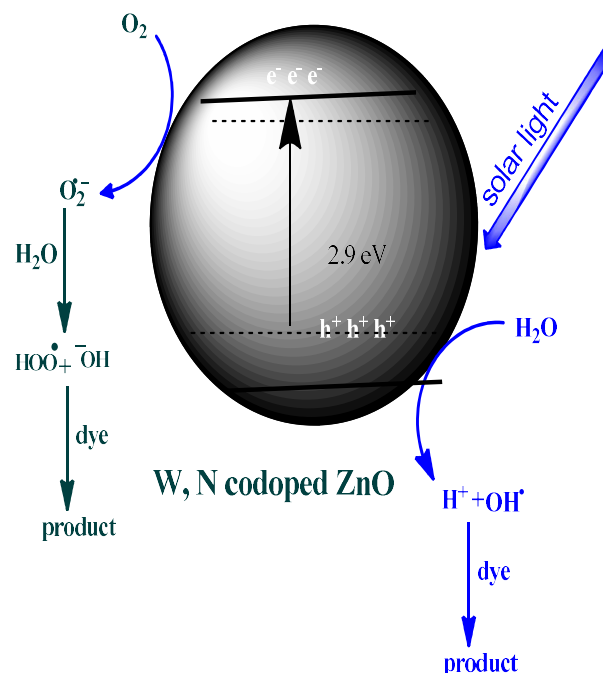
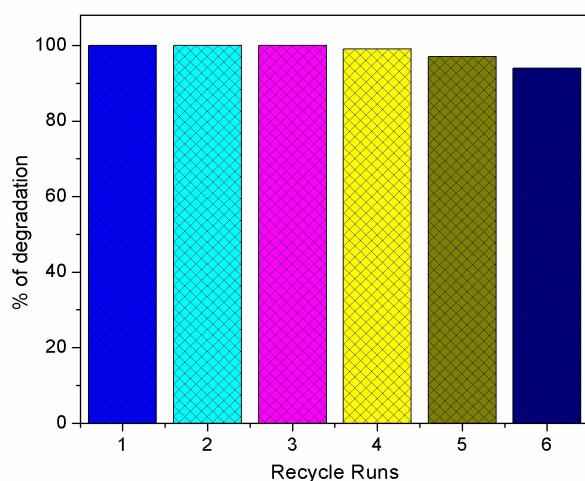


Figure - 7: Proposed electron-hole charge separation mechanism.

### 3.2.3 Reusability of the photocatalyst

Reusability is a very important parameter in assessing the practical application of photocatalysts in wastewater treatment<sup>[34]</sup>. It can contribute significantly to lowering the operational cost of the process. Hence the reusability of the 0.04 mol% W, N codoped ZnO was studied for the degradation of 50 mg l<sup>-1</sup> RB 4 solution at pH 5. The photocatalyst was carefully separated from the degraded dye solution by centrifugation and added to the fresh 100 ml dye solution. The results of the analysis were shown in **Figure 8**. It has been found that 0.04 mol% W, N codoped ZnO completely degraded the RB 4 solution in 120 minutes even in its third reuse, this shows that the composites have good stability in the acidic conditions. Hence application of 0.04 mol% W, N codoped ZnO for the treatment of textile effluents will be cost effective.



**Figure - 8: Reusability test on RB 4 over 0.04 mol% W, N codoped ZnO.**

### 3.2.4. Effect of pH of the dye solution on W, N-codoped ZnO

The pH of solutions significantly affects the reaction rates of semiconductor due to its persuade on surface charge properties of the photocatalysts. In **Figure 9** shows the photodegradation of RB 4 in the presence of optimized 0.04 mol% W, N-codoped ZnO was studied in the pH range 3-12. The concentration of dye solution was 50 mg/l, and the dosage of the photocatalyst was 0.5 mg/l. For pH > PZC the surface is negatively charged and pH < PZC the surface is positively charged. It should be noted the pH<sub>pzc</sub> of ZnO is 8.80<sup>[35]</sup>. The pH of the particle is neutral were called point of zero charge (PZC). The effect of pH on the photocatalytic activities can thus be understood in terms of electrostatic interactions between dye solution and the catalyst surface. This gorgeous interaction is moderately beneficial to increase the encounter probability of the hydroxyl radicals with RB 4 and increase the photocatalytic efficiency, while the repulsive

interaction would hinder the overall reaction. The photocatalysts are positively charged at pH bellow 7. Therefore, in the pH range 3-7 the positively charged 0.04 mol% W, N-codoped ZnO and the negatively charge RB 4 should readily attract each other, while they should repulse each other when pH is above 7 due to both are (0.04 mol% W, N-codoped ZnO and RB4) shows negative charge. As expected, the degradation rate at the optimal condition was found at around pH 5.

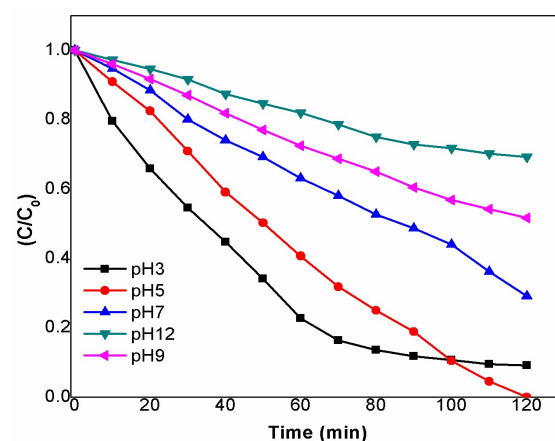


**Figure - 9: Effect of initial pH of dye on photocatalytic degradation**

The parent photocatalyst such as ZnO has followed the same mechanism, but at extreme pH values, such as pH 3 and 12 the ZnO gets readily dissolved. In an acidic and basic environment, ZnO nanoparticles exhibit a tendency to dissolve:



Therefore, the decreased photocatalytic activity at low and higher pH values can be attributed to the dissolution in strong acidic or alkaline environment.

### 3.2.5. Effect of dosage of the photocatalyst

To determine the effect of the catalyst loading, a series of experiments were carried out by varying the amount of catalyst from 25 to 150 mg L<sup>-1</sup>. The percentage of RB 4 degraded in 120 minutes for various catalyst dosages were given **Figure 10**. It can be observed that the efficiency of the photocatalytic degradation of RB 4 increases with the increase of the photocatalyst amount from 25 to 150 mg L<sup>-1</sup>. The enhancement of the removal efficiency on increase of the dosage of photocatalyst was due to the increase of active sites available for the photocatalytic reaction.

Rise of photocatalyst quantity above the optimum level gave rise to more important spectacles of light screening and scattering, decreasing the penetration depth of the light into

the suspension. Consequently, the overall number of photons reaching the photocatalyst surface decreased.

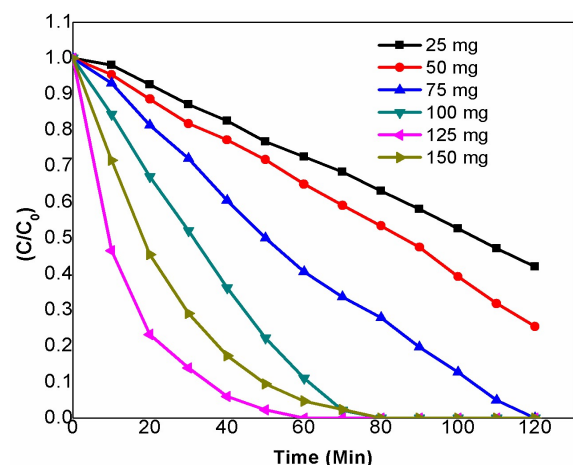


Figure - 10: Effect of dosage of the photocatalyst

### 3.2.6. Chemical Oxygen Demand (COD) analysis

The Chemical oxygen Demand test is widely used as an effective technique to measure the organic load in the wastewater and also to estimate the degree of mineralization of organic pollutant in water treatment. The analysis measure the organic load present in the water in terms of the total quantity of oxygen required to oxidize them to CO<sub>2</sub> and water. The reduction in COD values of the RB 4 solution before and after the treatment was estimated. Table 2 gives the percentage of degradation of dye calculated from spectrophotometric data and COD values for ZnO and W, N-codoped ZnO. The reduction in COD values of the treated dye solution indicates that the dye solution was not only decolourised but also mineralized into smaller molecules like CO<sub>2</sub>, NO<sub>2</sub> and so on. The mineralisation of RB 4 has lower percentage than the degradation; it might be due to the presence of triazine groups, which are reported chemically more stable than phenyl groups<sup>[36]</sup>.

Table - 2: COD analysis of the degraded Reactive Blue solution (Irradiation time: 2 hrs)

Photocatalysts	Reactive Blue 4	
	% degradation	% of reduction in COD
ZnO	100	66
W, N codoped ZnO	100	71

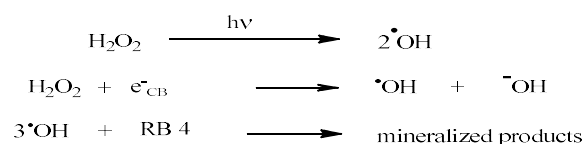
### 3.2.7 Effect of Oxidants on W, N codoped ZnO powder

Photocatalytic efficiency of W, N codoped ZnO was evaluated from their activity in the degradation of organic reactive dyes in solar light radiation.

Codoped ZnO powders are being effectively used to degrade many organic pollutants present in aqueous systems. The reason for the increased interest in this particular process is nothing but utilizing atmospheric molecular oxygen as an oxidant under usual conditions and inhibited electron-hole recombination centers. However, an oxygen molecule is incapable to abstract all the photo excited electrons because it has lower photocatalytic reduction potential<sup>[37]</sup>. Hence, the photocatalysts need very sufficient electron acceptors. However, irreversible electron acceptors (green oxidants) such as KBrO<sub>3</sub>, H<sub>2</sub>O<sub>2</sub> and (NH<sub>4</sub>)<sub>2</sub>S<sub>2</sub>O<sub>8</sub> supported to the oxygen molecule for the degradation of dye solution. This green oxidants can be produce the powerful oxidizing species such as BrO<sub>3</sub><sup>-</sup>, ·OH and SO<sub>4</sub><sup>-</sup>. These oxidizing species utilized the more photogenerated electrons than the O<sub>2</sub><sup>2-</sup> species due to it has a higher reduction potential. So that, its also contribute to reduce the recombination of the electron-hole pair's charges<sup>[37]</sup>. Therefore, we have studied the effect of electron acceptors such as hydrogen peroxide on the photocatalytic degradation of the RB 4.

#### 3.2.7.1. Effect of Hydrogen Peroxide (H<sub>2</sub>O<sub>2</sub>) Concentration

The oxidant combined heterogeneous photocatalytic degradation of RB 4 has been studied at different H<sub>2</sub>O<sub>2</sub> concentrations and the results are summarized in Figure 11. The removal efficiency of RB 4 increased with increasing the concentration up to 10 mM. For higher concentrations, no considerable improvement was observed. The higher photocatalytic degradation efficiency can be attributed to the increase of the concentration of hydroxyl radicals generated by photolytic peroxidation and photoexcited charges as shown in the following equations



At the highest concentrations, the reaction between H<sub>2</sub>O<sub>2</sub> and strong oxidant ·OH radicals and/or h<sub>vb</sub><sup>+</sup> became more relevant and as a consequence no subsequent improvement on the oxidant combined photocatalytic reaction rate can be noticed because the produced HO<sub>2</sub> (hydroperoxyl radicals) are less reactive than both hydroxyl radicals and h<sub>vb</sub><sup>+</sup><sup>[37]</sup>

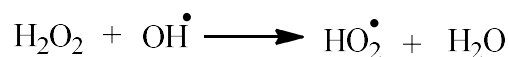
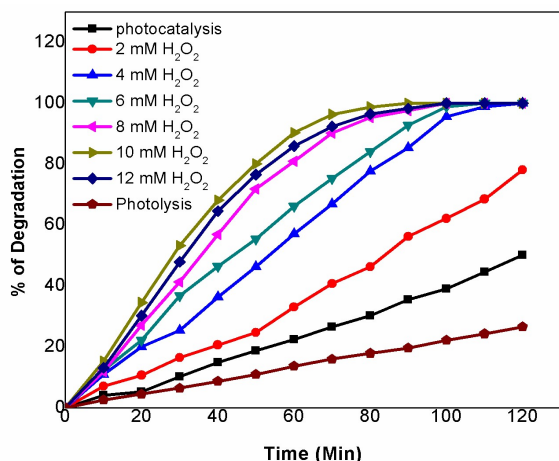


**Figure - 11:** Effect of concentration of H<sub>2</sub>O<sub>2</sub> on the efficiency of degradation of RB 4

(Initial concentration C<sub>0</sub>= 100 mg l<sup>-1</sup>, pH=5, Photocatalyst dosage 1 g l<sup>-1</sup>)

#### 4. CONCLUSION

Pure ZnO and W, N codoped ZnO powder prepared in co precipitation method followed by thermal treatment at 500°C for 5 hours has shown good activity for the degradation of reactive dyes in solar light. The prepared photocatalyst characterized by various techniques and also compared them photocatalytic activity. 0.04 mol% W, N codoped ZnO demonstrated highest activity for the degradation of RB 4 with a chlorotriazine functional group. The rate of degradation of RB 4 over W, N codoped ZnO was maximum when the solution pH was 5, and the dosage of the photocatalyst was 1 g l<sup>-1</sup>. A hydrogen peroxide concentration of 10 mM was found to be optimum for the achieving the maximum activity in a oxidant combined Photocatalytic process. The 0.04 mol% W, N codoped ZnO also has good reusability; the 0.04 mol% W, N codoped ZnO completely degraded RB 4 in 120 minutes in the oxidant combined photocatalytic process even in its fourth reuse. Hence oxidant combined photocatalytic process over 0.04 mol% W, N codoped ZnO will be an efficient and cost effective method for the degradation of organic dyes and other organic pollutants in industrial effluent.

#### 5. REFERENCES

1. M.A. Khan, A.M. Ghouri, Res. World J. Arts Sci. Commer. 2 (2011) 276.
2. B. Lellis, C.Z. Fávaro-Polonio, J.A. Pamphile, J.C. Polonio, Biotechnol. Res. Innov. 3 (2019) 275.
3. M.M. Hassan, C.M. Carr, Chemosphere 209 (2018) 201–219.
4. D. Fabbri, M.J. López-Muñoz, A. Daniele, C. Medana, P. Calza, Photochem. Photobiol. Sci. 18 (2019) 845–852.
5. D.W. Zelinski, T.P.M. dos Santos, T.A. Takashina, V. Leifeld, L. Igarashi-Mafra, Water. Air. Soil Pollut. 229 (2018) 1–12.
6. E. Regulska, D. Rivera-Nazario, J. Karpinska, M. Plonska-Brzezinska, L. Echevoyen, Molecules 24 (2019) 1118.
7. S.A. Ansari, S.G. Ansari, H. Foad, M.H. Cho, New J. Chem. 41 (2017) 9314–9320.
8. A. Naldoni, F. Riboni, U. Guler, A. Boltasseva, V.M. Shalaev, A.V. Kildishev, Nanophotonics 5 (2016) 112.
9. U. I. Gaya, A. H. Abdullah, J. Photochem. Photobiol. C, 9 (2008) 1-12.
10. J. M. Herrman, Catalysis Today, 53 (1999) 115-129.
11. C. Shifu, Z. Wei, Z. Sujuan, L. Wei, Chem. Eng. J., 148 (2009) 263–269.
12. D. Chatterjee, D. Shimanti, Photochem. Rev., 6 (2005) 186-205.
13. S. Sakthivel, M. Janczarek, H. Kisch, J. Phys. Chem., 108 (2004) 19384-19387.
14. M. Pera-Titus, V. García-Molina, M. B̃anos, J. Giménez, S. Esplugas, Appl. Catal. B Environ., 47 (2004) 219-256.
15. U. Poornaprakash, K. Chalapathi, S.V. Subramanyam, Y. Prabhakar Vattikuti, S.P. Shun, Mater. Res. Express 6 (2019) 105356.
16. B. Poornaprakash, U. Chalapathi, P.T. Poojitha, S.V.P. Vattikuti, M.S.P. Reddy, J. Mater. Sci. Mater. Electron. 30 (2019) 9897–9902.
17. M. Kaur, A. Umar, S.K. Mehta, S. Singh, S.K. Kansal, H. Fouad, O.Y. Allothman, Material 11 (2018) 2254.
18. C. Díaz-Urbe, J. Vilorio, L. Cervantes, W. Vallejo, K. Navarro, E. Romero, C. Quiñones, Int. J. Photoenergy 2018 (2018) 1–8.
19. B. Poornaprakash, U. Chalapathi, P.T. Poojitha, S.V.P. Vattikuti, S.H. Park, J. Supercond. Nov. Magn. 33 (2020) 539–544.
20. C. Diaz-Urbe, W. Vallejo, G. Camargo, A. Muñoz-Acevedo, C. Quiñones, E. Schott, E. X. Zarate, J. Photochem. Photobiol. A Chem. 2019, 384, 112050.
21. D.G. Fan, R. Zhang, Y. Li, Solid State Commun. 39 (2010) 1911–1914.
22. S. Kumar, A. Baruah, S. Tonda, B. Kumaret, V. Shanker, B. Sreedhar, Nanoscale 9 (2014) 4830–4842.

23. R. Asahi, T. Morikawa, T. Ohwaki, K. Aoki, Y. Taga, Visible-light photocatalysis in nitrogen-doped titanium oxides, *Science* 5528 (2001) 269–271.
24. X. Yang, A. Wolcott, G. Wang, A. Sobo, R.C. Fitzmorris, F. Qian, J.Z. Zhang, Y. Li, *Nano Lett.* 6 (9) (2009) 2331–2336.
25. H. Schulz, K.H. Thiemann, *Solid State Commun.*, 32 (1979) 783
26. A.R. Babar, P.R. Deshamukh, R.J. Deokate, D. Haranath, C.H. Bhosale, K.Y. Rajpure, *Journal of Physics D: Applied Physics* 41 (2008) 135404.
27. L. Xu, X. Li, *Journal of Crystal Growth* 312 (2010) 851–855
28. K. J. Kim and Y. R. Park, *Journal of Applied Physics*, 96 (2004) 4150–4153
29. P. Wu, N. Du, H. Zhang, L. Jin and D. Yang, *Mater. Chem. Phys.*, 2010, 124, 908.
30. Khana, S.A.; Noreen, F.; Kanwal, S.; Iqbal, A.; Hussain, G. *Mater. Sci. Eng. C* 2018, 82, 46–59.
31. Zheng, Y.; Chen, C.; Zhan, Y.; Lin, X.; Zheng, Q.; Wei, K.; Zhu, J.; Zhu, Y. *Inorg. Chem.* 2007, 46, 6675–6682.
32. M.M. Mohamed and M.M. Al-Esaimi, *Journal of Molecular Catalysis A: Chemical* 255 (2006) 53
33. B. Naik, K.M. Parida, *Industrial and Engineering Chemistry Research* 49 (2010) 8339-8346
34. I.K. Konstantinou, T.A. Albanis, *Applied Catalysis B: Environmental* 42 (2003) 319-335
35. J. Zhao, T. Wu, K. Wu, K. Oikawa, H. Hidaka and N. Serpone, *Journal of Environmental Science Technology* 32 (1998) 2394.
36. A.B. Prevot, M. Vincenti, A. Bianciotto and E. Pramauro, *Appl. Catal. B: Environ.* 22 (1999) 149
37. D. Robert, B. Dongui and J.V. Weber, *J. Photochem. Photobiol. A: Chem.* 156 (2003) 195.